

Pulse transit time estimation methods in a novel arterial simulator with variable pulse wave velocity

Federico Filippi¹, Giorgia Fiori¹, Gabriele Bocchetta¹, Vincenzo La Battaglia¹, Stefano Marini¹, Salvatore Andrea Sciuto¹, Andrea Scorza¹

¹ Department of Industrial, Electronic and Mechanical Engineering, Roma Tre University, Via della Vasca Navale 79, 00146 Rome, Italy

ABSTRACT

Arterial stiffness is one of the key indicators of cardiovascular diseases, for which an early identification is crucial. Pulse Wave Velocity (PWV) is a widely used parameter to assess arterial stiffness. In clinical practice, it is common use to measure the PWV through the estimation of the Pulse Transit Time (PTT). In this study a comparison among three PTT estimation methods (peak-to-peak, tangent-secant, and cross-correlation) is proposed and applied to waveforms acquired on a novel arterial simulator able to change the stiffness of an arterial surrogate by varying the transmural pressure. After a measurement campaign carried out for several pressure values, the cross-correlation method has been confirmed to be the most robust, with uncertainties below 1.3 %. The operating principle of the arterial simulator has been confirmed since a change in transmural pressure of 25 kPa resulted in a change in PWV mean values of up to 1.7 m/s.

Section: RESEARCH PAPER

Keywords: Pulse wave velocity; pulse transit time; arterial simulator; arterial stiffness; cross-correlation

Citation: F. Filippi, G. Fiori, G. Bocchetta, V. La Battaglia, S. Marini, S. A. Sciuto, A. Scorza, Pulse transit time estimation methods in a novel arterial simulator with variable pulse wave velocity, Acta IMEKO, vol. 13 (2024) no. 4, pp. 1-8. DOI: [10.21014/actaimeko.v13i4.1782](https://doi.org/10.21014/actaimeko.v13i4.1782)

Section Editors: Luca Callegaro, INRiM, Italy, Jakub Svatos, CVUT Prague, Czech Republic, Platon Sovilj, University of Novi Sad, Serbia, Jan Saliga, Technical University of Kosice, Slovakia

Received February 18, 2024; **In final form** June 17, 2024; **Published** December 2024

Copyright: This is an open-access article distributed under the terms of the Creative Commons Attribution 3.0 License, which permits unrestricted use, distribution, and reproduction in any medium, provided the original author and source are credited.

Corresponding author: Federico Filippi, e-mail: federico.filippi@uniroma3.it

1. INTRODUCTION

Detecting the change in arterial stiffness is of paramount importance because it can reveal the early onset of cardiovascular diseases (CVDs) before their typical symptoms become apparent. Some examples in which an increase in stiffness of the large elastic arteries occurs are in the presence of hypertension, diabetes mellitus, atherosclerosis, hypercholesterolemia, and isolated systolic hypertension that afflicts the elderly population. [1]-[6]. Since CVDs are acknowledged by the World Health Organization as the leading cause of death in the world [7], continuous research and refinement of methods for the assessment of arterial stiffness is fully justified.

Over the years, the relationship between arterial stiffness and other hemodynamic quantities has been investigated [8]. In particular, it has been shown to influence the speed of propagation of pressure waves, generated by the heartbeat, within blood vessels, better known as Pulse Wave Velocity (PWV) [9]. Nowadays, Pulse Wave Velocity (PWV) is a widely used and well-established parameter to assess arterial stiffness and, consequently, the health status of the cardiovascular system

[10]-[12]. In fact, its measurement can be carried out with non-invasive techniques [13], making it a simple and patient-friendly practice and is used as a significant predicting marker for cardiovascular risk assessment and as a metric to evaluate the success of a specific treatment. In clinical practice, it is common use to measure the PWV through the estimation of the Pulse Transit Time (PTT) defined as the difference between the time instants in which the pulse pressure wave, produced by the heartbeat, passes through two different sites of the arterial tree [13].

Many procedures have been implemented to evaluate the PTT and some of them turn out to be more reliable than others depending on the setup conditions and the quality of acquired signals [14]-[21]. Traditionally, these methods are based on the evaluation of the time lag between some characteristic points of pressure waveforms [14], [16], [17]. Some of the most well-known include the maximum peak, the minimum peak, the maximum of the second derivative, and the foot of the wave calculated through the intersecting tangent method, considered in the literature as the gold standard [17]. The comparison

between these methods has been carried out in the scientific literature on both simulated waves [14], [15] and signals acquired on human bodies [16], [17], highlighting how PTT is highly dependent on the chosen method due to arbitrariness in selecting the characteristic points. To overcome this issue, other methods for measuring PTT have been investigated. Among them, the cross-correlation technique has been widely used since it takes into account the entire waveform evolution and can be used to evaluate a sequence of waves simultaneously [18]-[21]. Specifically, in [20], a cross-correlation-based method was compared with two point-based methods in estimating PWV on healthy patients and found to have a better intra-observer repeatability and a superior inter-test reproducibility.

To better understand how pulse waves propagate within ducts, to study the relationship between PWV and other hemodynamic quantities, and also to experimentally validate the mathematical models describing the phenomenon, arterial simulators have been used [22]-[26] since they can reproduce the behavior of the cardiovascular system with the advantage of isolating and studying the phenomena of interest [27]. Although these simulators have different configurations based on the phenomenon to be reproduced, they are usually based on the same main components: (a) a real vessel or an arterial surrogate (AS) connected to a hydraulic circuit, (b) a pumping system able to generate pulse waves and (c) a sensing system for detecting the transit of the pulse wave inside the vessel [27]. Among them, simulators developed to specifically evaluate the relationship between PWV and compliance can be found [28]-[31]. Recently, an arterial simulator has been proposed to simulate changes in arterial stiffness by pre-tensioning the rubber hose that constituted the AS [32]. In [33], another experimental setup has been implemented with the same purpose. In this case, the arterial stiffness change has been simulated by acting on the AS tensioning state by varying its transmural pressure, i.e., the difference between the pressure inside and outside the vessel. It is worth noting that the outcomes in [33] are affected by the limited variation in external pressure taking off the possibility of analyzing the effect of various stress-strain conditions.

Although the use of arterial simulators is a well-established practice, the reliability of measurement methods to assess PTT on them is lacking in the literature. This aspect, however, is crucial since the waveforms produced within the arterial simulators are different from those of the human body given the presence of intrinsic differences, e.g., different materials that respond differently to the passage of pulse waves, presence of components connecting the AS to the apparatus that inevitably generate multiple reflections of the pressure wave.

Based on the abovementioned considerations, some of the methods used in the literature for the PTT evaluation have been applied in this work to waveforms acquired on a novel arterial simulator. The latter is able to change the stiffness of an AS to induce a change in PWV by varying the transmural pressure, with mean pressure up to three times higher than the atmospheric one. This apparatus provides an experimental tool that will be used for a deeper understanding of how the tensional state of the AS, due to transmural pressure, affects its ability to transmit the pressure wave. For this purpose, a measurement campaign has been carried out on the arterial simulator by setting different transmural pressure values. The acquired waveforms, after being conditioned, have been processed with three methods for PTT estimation.

In Section 2 the experimental setup, the measurement chain, and the waveform conditioning are described together with the PTT evaluation methods applied. In Section 3 the measurement uncertainty analysis is carried out. In Section 4, the results are presented and discussed focusing on the comparison among the tested methods. Finally, in the final section conclusions and future developments are outlined.

2. MATERIALS AND METHODS

2.1. The arterial simulator

The arterial simulator used in this work is based on the same working principle in [34]: varying the stress-strain state of the arterial surrogate, it is possible to change its distensibility, i.e., the ability of the vessel to vary its area (dA) in relation to the internal pressure changes (dp) given by the heartbeat. This results in a variation of PWV, according to the Bramwell-Hill equation [9]:

$$PWV = \sqrt{\frac{A}{\rho} \cdot \frac{dp}{dA}}, \quad (1)$$

where A is the cross-sectional area of the vessel and ρ is the density of the inner fluid. The distensibility is associated to the term:

$$\chi = \frac{dA}{A \cdot dp}. \quad (2)$$

By combining (1) and (2), the relationship between the PWV and the distensibility can be found:

$$PWV = \sqrt{\frac{1}{\rho \cdot \chi}}. \quad (3)$$

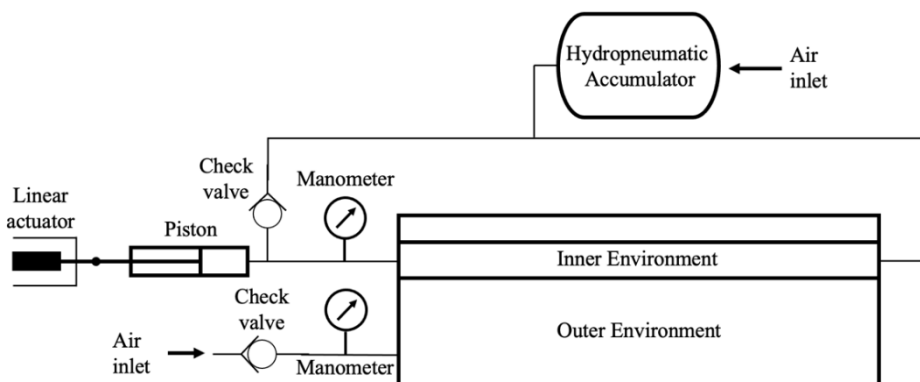


Figure 1. Principal components of the arterial simulator.

According to [9], distensibility, as defined in (2), can be related to the elastic modulus and geometric dimensions of the blood vessel, or its surrogate, according to the following formula:

$$\chi = \frac{D}{E \cdot t}, \quad (4)$$

where D is the internal diameter, t is the thickness and E is the elastic modulus of the vessel. The stress-strain condition on the AS walls is varied by acting on the difference between internal and external pressures (p_{in} and p_{out} , respectively) of the AS, known as transmural pressure (ΔP):

$$\Delta P = p_{in} - p_{out}, \quad (5)$$

ensuring that p_{in} is always higher than p_{out} to avoid AS collapse.

Compared to [34], the experimental setup consists of similar components with some improvements in the hydraulic circuit and in the actuation system (Figure 1). As in the previous version, a silicon rubber hose, representing the AS (Table 1), is filled with a fluid (i.e., distilled water) and connected to a piston that generates the pulse waves. A hydro-pneumatic accumulator is used for changing internal pressure: it contains an air chamber separated from the hydraulic circuit by a membrane; through insufflations of air, it is possible to change the air pressure and consequently also the pressure of the fluid within the system. The air chamber, containing an elastic fluid, is also useful for dissipating pressure waves so as to reduce multiple wave reflections. The AS is closed in a polymethyl methacrylate case, filled with air, so the external pressure can be changed. During the installation inside the case, the AS is pre-tensioned in order to remove the deflection caused by the force of gravity. Both pressures are continuously monitored with two digital manometers (Keller 23SY). Some components have been added to the setup compared to the previous version. A different hose, made of polyvinyl chloride (PVC), is connected in a closed loop with the inlet and the outlet of the AS to let the working fluid flow through the surrogate. It is a flexible tube with viscoelastic behavior that allows it to dissipate the pressure wave and prevent it from re-entering the aortic surrogate; however, it is stiffer than silicone rubber and thus can withstand the working pressures expected by the system without visibly deforming (compared with silicone rubber). The length of the PVC hose (3 m) is greater than that of the AS to allow the dissipation of reflections. Moreover, the different material allows it to withstand pressures higher than ambient pressure without deforming. Finally, a linear actuator drives the piston to ensure the repeatability of the pulse wave generation.

2.2. Waveforms acquisition and conditioning

To detect the transit of the pulse wave, two strain gauges (Micro-Measurement CEA-06-240UZ-120) have been glued with cyanoacrylate on the AS at a known distance, $\Delta L = (25.0 \pm 0.1)$ cm. Each strain gauge was connected in a quarter-bridge configuration to a channel of a strain gauge conditioner (Vishay

Table 1. Main characteristics of the silicon rubber hose used as arterial surrogate. Values are expressed as mean \pm standard deviation (SD).

Characteristic	Value
Length (cm)	42.0 \pm 0.1
Inner diameter (mm)	16.0 \pm 0.4
Thickness (mm)	2.0 \pm 0.1
Pre-tensioning (cm)	1.0 \pm 0.2

Table 2. Main settings of the DAQ board.

Characteristic	Nominal Value
Channel sample rate (kHz)	100
Signal length (s)	1.5
Number of channels	2
Voltage range (mV)	[-200; 700]

2120A) containing a Wheatstone bridge. The amplifier gain of both channels was set to the same value. The output signals from the conditioner have been connected, through BNC cables, to a DAQ board (NI USB-6251) for the acquisition of the strain gauge signals. An in-house NI LabView software has been implemented to process and store the signals. The main DAQ settings for data acquisition are listed in Table 2. The sample rate value has been chosen taking into account the distance between the strain gauges which requires a high temporal resolution to clearly distinguish PTT variations of 0.1 ms. The value of the signal length was chosen to ensure the acquisition of the entire transient phenomenon (pressure wave passage). The voltage range was selected taking into account the value set for the amplifier and the strain gauge strain magnitude, to take advantage of the full available resolution of the DAQ.

A measurement campaign has been carried out to validate the working principle of the arterial simulator (Table 3). Keeping the external pressure fixed, the internal pressure has been varied in steps to cause a change in transmural pressure: this procedure has been adopted to more closely mimic what happens in the human body where the pressure imposed from outside can reasonably be considered constant while the internal pressure of the vessels can vary according to the health condition of the individual. A total of ten acquisitions have been performed for each ΔP value. This procedure has been repeated for three different external pressures. The maximum transmural pressure value ($\Delta P_{max} = 25$ kPa) reached was determined experimentally: laboratory tests showed that for values $\Delta P > 25$ kPa the bonding tightness between strain gauges and AS is no longer guaranteed probably due to the dilation differences between the materials of the two components. The minimum value of ΔP taken into consideration is $\Delta P_{min} = 0$ kPa ($p_{in} = p_{out}$) to avoid the collapse of the AS. The ΔP values were chosen by ensuring that a significant difference among them is provided also by taking into account the nominal uncertainty of the gauges (± 1.3 kPa): the uncertainty of each ΔP is given by the sum in quadrature of the type B uncertainties declared for each gauge (± 1.8 kPa) as type A contribution is considered negligible. Finally, six pressure values were selected taking into account the upper and lower limits determined above. The outer pressure maximum value has been imposed by paying attention to the maximum force that can be applied by the linear actuator. The piston used to generate the pressure pulse, being connected to the circuit externally to the external case, senses on one side the ambient pressure and on the other one the pressure inside the hydraulic circuit, which is given, as a first approximation, by the sum of the absolute values of the p_{in} and p_{out} applied on the walls of the AS [8]. The higher the absolute pressure inside the vessel, the more the piston resists displacement and consequently the more force the linear actuator must exert to move the piston and generate the impulse. Preliminary tests have shown that above 250 kPa (absolute pressure) the actuator cannot generate the right pressure pulse. Having defined the lower and upper limits of ΔP and p_{out} , the

Table 3. Parameter settings for the measurement campaign. Pressure values are expressed as gauge pressure. All values are expressed as mean \pm standard deviation (SD).

Parameter	Setting
Outer pressure (kPa)	(50.0 to 150.0) \pm 1.3
Outer pressure steps (kPa)	50.0 \pm 1.3
Transmural pressure (kPa)	(0.0 to 25.0) \pm 1.3
Transmural pressure steps (kPa)	5.0 \pm 1.3
System temperature ($^{\circ}$ C)	22.0 \pm 0.5

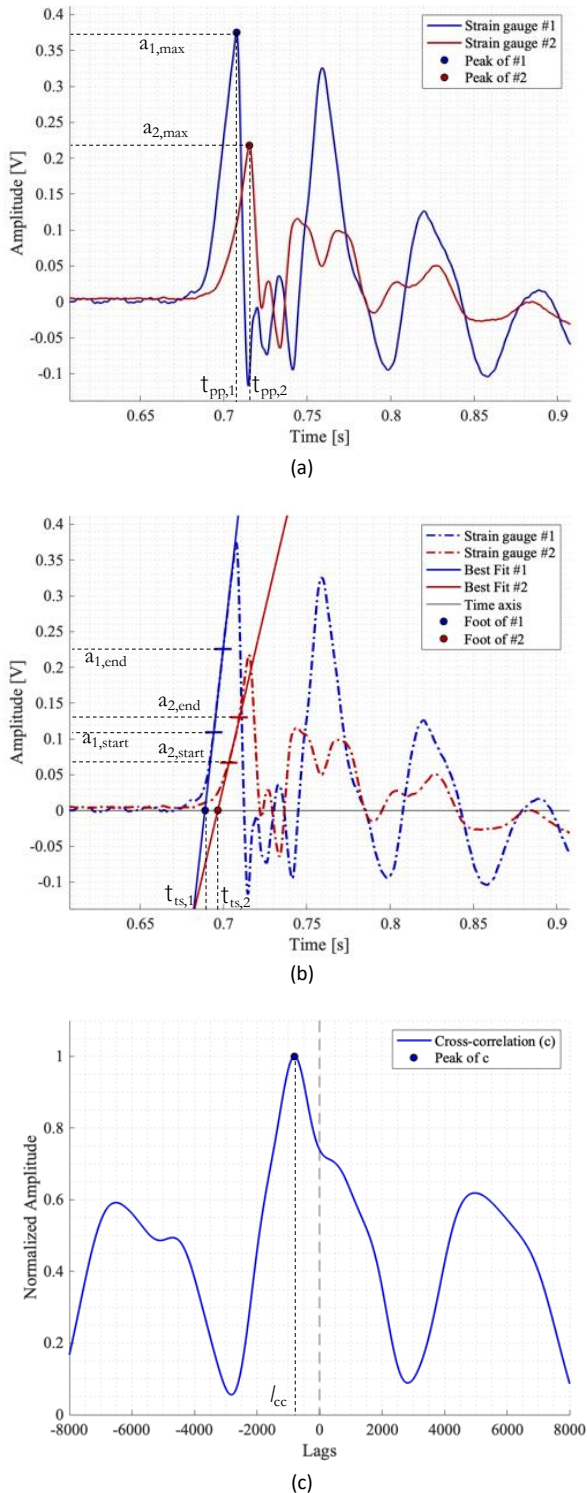


Figure 2. Example of the working principle of each method: (a) peak-to-peak method, (b) tangent-secant method, (c) cross-correlation method.

range of the internal pressure p_{in} can be determined from (4). Since PWV, and consequently PTT, also depends on the density of the inner fluid (1), the environment temperature has been monitored and kept constant through an air conditioning system during the measurement campaign. Temperature control is important, also, because it affects the mechanical characteristics of AS and the operation of electronic devices (e.g., measuring chain).

After the acquisition phase, a spectral analysis has been conducted, through the Fast Fourier Transform function in MATLAB, to assess the signal frequency content: through a zero-phase digital filtering technique [35], a Butterworth low-pass filter (1st order – cut-off frequency: 150 Hz) has been applied to remove high-frequency contributions related to noise, and a Butterworth notch filter (1st order – stop-band frequencies: 49-51 Hz) has been applied to cut off the 50 Hz noise due to power grid interference.

2.3. PTT evaluation methods

For the PTT evaluation, the waveforms acquired from the simulator have been processed by MATLAB software, implementing three different methods known in literature [14]-[21] and discussed below: the peak-to-peak method (PP), the tangent-secant method (TS) and the cross-correlation method (CC).

The peak-to-peak method estimates the PTT by evaluating the difference between the two time instants ($\tau_{pp,1}$ and $\tau_{pp,2}$) at which the maximum peak of the two pressure waves occurs. Figure 2a shows an example of two acquired pressure signals in which the two peaks ($a_{1,max}$ and $a_{2,max}$) for the PTT estimation by the PP method have been identified.

The tangent-secant method evaluates the PTT by calculating the time distance between the waveforms' feet. In particular, two straight lines are identified, representative (ideally, tangents) of the inclination of the positive slope of their respective pulse wave. To locate the lines, linear regression procedure is performed on a specific interval of the waveforms' upstroke identified by two values corresponding to a fraction of the maximum value of the waves. In particular, the interval has been chosen between 30 % and 60 % of the maximum, thus obtaining:

- $a_{start} = 0.30 \cdot a_{max}$
- $a_{end} = 0.60 \cdot a_{max}$

The foot of the waveforms has been identified in time by the intersection between the lines and the time axis. Similarly to the previous case, Figure 2b shows the above pressure signals that have been processed by the TS method. The two tangent lines, passing through a_{start} and a_{end} , allow identifying the waveform feet ($\tau_{ts,1}$ and $\tau_{ts,2}$) for the PTT estimation.

Finally, the cross-correlation method is usually used to evaluate the similarity degree of two waveforms. By applying this method to the waveforms, the second is shifted along the time axis step by step (one step is called lag – one lag corresponds to one sample), then, the integral of the product between the two waveforms is calculated for each position. In the cross-correlation function, the number of lags (l_{cc}) that separate the peak from zero multiplied by the sampling period represents the time distance ($\Delta\tau_{cc}$) between the two waveforms, i.e., the PTT. Figure 2c shows the curve representing the cross-correlation between the two pressure signals, where the peak corresponding to their phase shift is identified, from which the PTT is estimated.

Table 4. Distribution characteristics of MCSs variables.

Variable	Distribution	Variability
Cut-off frequency (Hz)	uniform	$f_c \pm 1$
PP time instants (ms)	uniform	$\tau_{pp} \pm 0.1$
TS interval limits (%)	uniform	$a_{start} \pm 1; a_{end} \pm 1$
CC lags	uniform	$l_{cc} \pm 1$

3. UNCERTAINTY ESTIMATION

The uncertainty associated with the PTT values for each test condition has been estimated by summing in quadrature the contribution due to signal processing through the implemented methods (σ_{met}) and the one due to the repeatability of measurements under the same conditions (σ_{rep}):

$$\sigma_{PTT} = \sqrt{\sigma_{met}^2 + \sigma_{rep}^2}. \quad (6)$$

For the estimation of the method uncertainty σ_{met} , a Monte Carlo Simulation (MCS) has been carried out for each acquisition, since it is well-known in the literature that this is a valid and robust tool for estimating uncertainties deriving from software-based measurement methods, following the approach adopted in [36]-[39]. First of all, a distribution has been assigned to the cut-off frequency (f_c) of the low-pass filter applied in the pre-processing phase of the acquired data. Consequently, a distribution has been assigned to the quantities involved in the methods to calculate the PTT. For the PP method, a distribution has been assigned to $\tau_{pp,1}$ and $\tau_{pp,2}$ to consider the issues due to the identification of the time instant relative to the peak of the wave. For the TS method, a distribution has been assigned to the extremal values of the intervals (a_{start} and a_{end}) used to determine the tangent lines. As regards the CC method, similarly to the PP method, a distribution has been assigned to the lag that identifies the maximum correlation between the two waves. Therefore, σ_{met} has been estimated as the standard deviation of the mean calculated considering the uncertainties related to the MCSs performed on the acquisitions under the same measurement conditions. In Table 4, the characteristics of the distributions assigned to the variables of interest for MCSs are listed.

On the other hand, for the estimation of the repeatability contribution to uncertainty σ_{rep} , the dispersion of the PTT values from 10 pressure waves acquired and processed under the same test conditions has been computed.

4. RESULTS AND DISCUSSIONS

In this section, the results of the PTT obtained with the three proposed methods for the different test conditions are presented and discussed. In Table 5, the results for increasing transmural pressure ΔP values for the three external pressure conditions are reported. The results are expressed in terms of mean \pm standard deviation (SD). The outcomes for the TS method are found to be compatible with the ones for the other two methods but they are characterized by the highest standard deviation values. The corresponding uncertainty is up to 10 %, 11 % and 23 % of the mean value, respectively for the measurements carried out with p_{out} of 50 kPa, 100 kPa and 150 kPa. The advantage of the TS method is that it is less affected by multiple reflections [16] since it focuses on the first part of the upstroke of the waveforms. However, the high uncertainty of results is likely due to the sensitivity of the method to tangent line slope. Indeed, a small gradient variation reflects in a non-negligible time-shifting of the foot of the waveforms. Since the waveform upstroke is also determined by other frequencies in addition to the characteristic one of the phenomena, the variability of the collected waves could cause a dispersion of the results higher than the other methods. As regards the PP and CC methods show less dispersion, although most of the results seem not compatible among them. The advantage of the PP method is its ease of implementation and low computational cost. However, the limitation of the technique is that the waveform is highly dependent on the choice of the measurement site [40] because (a) the waveform may change its shape given dissipations due to viscoelastic effects and (b) reflections, which are generated close to vessel bifurcations or occlusions, return back and overlap with the direct wave. Therefore, the peak of the resulting wave may differ in time position and amplitude from that of the single direct wave. Thus, even if the method provides a narrow uncertainty, almost constant and below 1.4 %, the resulting average values may deviate from the true values, since the shape of the second waveform is different from the first one. Distortion in the shape of pressure waves is a problem that also affects the CC method [41]. To avoid the influence of wave distortions due to reflections, CC is used in the literature by considering only the ramp-up, but from laboratory tests, we found that the results are highly dependent on the foot of the wave considered. Therefore, in this study as in [20], also given the small distance between the two measurement sites, it is assumed, in agreement with [40], that the contribution of this effect is negligible compared to the same contribution for the PP method, and then the whole wave is considered for PTT calculation with this method. Further investigation needs to be conducted about the choice of the wave portion taken into consideration. The uncertainty values (standard uncertainty) of PTTs deriving from CC method application, are almost constant

Table 5. PTT Results expressed in milliseconds, in terms of mean \pm SD.

ΔP (kPa)	$p_{out} = 50$ kPa			$p_{out} = 100$ kPa			$p_{out} = 150$ kPa		
	PP	TS	CC	PP	TS	CC	PP	TS	CC
0	7.4 \pm 0.1	7.5 \pm 0.5	7.6 \pm 0.2	7.4 \pm 0.1	8.0 \pm 0.6	7.9 \pm 0.1	7.5 \pm 0.1	7.0 \pm 0.6	8.0 \pm 0.1
5	7.3 \pm 0.1	7.2 \pm 0.5	7.5 \pm 0.1	7.6 \pm 0.1	7.4 \pm 0.4	8.0 \pm 0.1	7.6 \pm 0.1	7.2 \pm 0.8	8.0 \pm 0.1
10	7.4 \pm 0.1	7.3 \pm 0.4	7.6 \pm 0.1	7.6 \pm 0.1	8.1 \pm 0.6	8.1 \pm 0.1	7.7 \pm 0.1	7.1 \pm 1.4	8.1 \pm 0.1
15	7.5 \pm 0.1	7.8 \pm 0.4	7.8 \pm 0.1	7.7 \pm 0.1	7.7 \pm 0.8	8.2 \pm 0.1	7.8 \pm 0.1	7.4 \pm 1.6	8.2 \pm 0.1
20	7.6 \pm 0.1	8.4 \pm 0.8	7.9 \pm 0.1	7.8 \pm 0.1	8.3 \pm 0.8	8.3 \pm 0.1	7.8 \pm 0.1	7.5 \pm 1.7	8.3 \pm 0.1
25	7.7 \pm 0.1	8.4 \pm 0.7	8.1 \pm 0.1	7.8 \pm 0.1	8.3 \pm 0.8	8.4 \pm 0.1	7.8 \pm 0.1	6.9 \pm 1.5	8.3 \pm 0.1

Table 6. Compatibility between the three methods. According to (7), green and red boxes indicate respectively the presence or the absence of compatibility between two results.

ΔP	$p_{out} = 50 \text{ kPa}$			$p_{out} = 100 \text{ kPa}$			$p_{out} = 150 \text{ kPa}$		
	PP-TS	TS-CC	CC-PP	PP-TS	TS-CC	CC-PP	PP-TS	TS-CC	CC-PP
0	Green	Green	Green	Green	Green	Red	Green	Red	Red
5	Green	Green	Green	Green	Green	Red	Green	Red	Red
10	Green	Green	Green	Green	Green	Red	Green	Red	Red
15	Green	Green	Green	Green	Green	Red	Green	Red	Red
20	Red	Green	Red	Green	Green	Red	Red	Red	Red
25	Red	Green	Red	Green	Green	Red	Red	Red	Red

and below 1.3 %. To evaluate the compatibility between the three methods results has been used the formula suggested by [42]:

$$|\mu_x - \mu_y| \leq \sigma_x + \sigma_y, \quad (7)$$

where x and y represent two of the three methods, μ and σ represent the mean value and the standard deviation of results in a specific test condition reported in Table 5, respectively. Compatibility is verified if inequality in (7) is met. Table 6 shows, for all test conditions in Table 5, the result of applying inequality (7) between the three methods. Specifically, a green box indicates that the inequality is met. On the contrary, a red box indicates that there is no compatibility between the results considered. In most cases, according to (7), the compatibility of the results is ensured for PP and TS methods but is not respected between CC and both other methods: in particular, as the external pressure increases, the mean values of CC move away from those of TS and PP. In general, the increasing trend in PTT mean values, for all the three methods, confirms an effective variation in PWV due to transmural pressure changes.

Building on the previous statements, it is worth noting that also the scientific literature confirms cross-correlation as a robust method for PTT assessment. This is further supported by its reproducibility even in the presence of noise in the acquired signals and in cases of reduced temporal resolutions [18]-[21], [41], [43]. Therefore, in the present study it has been considered the best of the three methods to evaluate the change in PWV within the aortic surrogate caused by the change in transmural

pressure, for different external pressures, to validate the working principle of the proposed arterial simulator. Figure 3 shows that, given the same external pressure, mean PWV values have a decreasing trend as ΔP increases. A ΔP variation of 25 kPa corresponds to a decrease in PWV mean values of 1.7, 1.5 and 0.9 m/s with an outer pressure of 50, 100 and 150 kPa, respectively. As regards the standard deviation of the measured PWV, is usually below 1 % of the mean value. Furthermore, the trend appears non-linear. This behavior appears compatible with the non-linear and decreasing trend of the elastic modulus of the silicone rubber as the stress-strain state changes [44]. For the early portion of its stress-strain curve, indeed, increasing strain induces a decrease in the elastic modulus. This behavior, with the deformation induced by the increase in transmural pressure within the AS, could result in a consequent increase in the distensibility of the duct causing a decrease in PWV, according to (1) and (4). In addition, it can be seen that for $\Delta P = 0$, while increasing the external pressure, PWV decreases. This is likely due to the greater pressure acting on the outer and inner walls of the duct inducing a compression state of the walls. To quantitatively justify the trend of PWV, the trend of the elastic modulus of the material as its deformation state changes should be known. This aspect will be explored in future developments.

5. CONCLUSIONS

In this work, three methods for the PTT estimation have been tested on a novel arterial simulator able to change the PWV of an arterial surrogate by changing the tensional state of its walls. In particular, the stress-strain condition can be modified by varying, independently, inner and outer pressures of the AS embedded in a sealed case filled with compressed air and connected to a hydraulic circuit loaded with water. A piston, driven by a linear actuator, generates the pressure pulses. Two strain gauges, glued on the AS to detect the pressure wave transit at different sites, have been connected to a measurement chain to acquire strain signals. Peak-to-peak, tangent-secant and cross-correlation methods have been applied to estimate the PTT of pulse waves resulting from a measurement campaign under different transmural pressure conditions. The measurement uncertainty has been estimated by combining the contribution due to repeatability, from repeated measurements under the same test conditions, and that due to the method, estimated through Monte Carlo simulations.

The results confirm the working principle of the arterial simulator showing a change in mean PWV values depending on the transmural pressure. Moreover, as already known in the literature, it is confirmed that cross-correlation is a robust method for PTT assessment. The study represents a step forward in the development of variable PWV arterial simulators, useful for calibrating, in the near future, medical devices for PWV assessment or as a support device in training medical technicians. In the future, it will certainly be necessary to investigate more thoroughly the effect that transmural pressure causes on the stress-strain state of the AS. In addition, it would be interesting to investigate the behavior of PWV in the duct for higher transmural pressure values by applying high-deformation strain gauges on the surrogate. In addition, the pressure pulse generation system could be changed (e.g., by using a peristaltic pump) to more closely reproduce the pseudo-periodic phenomenon of heartbeat.

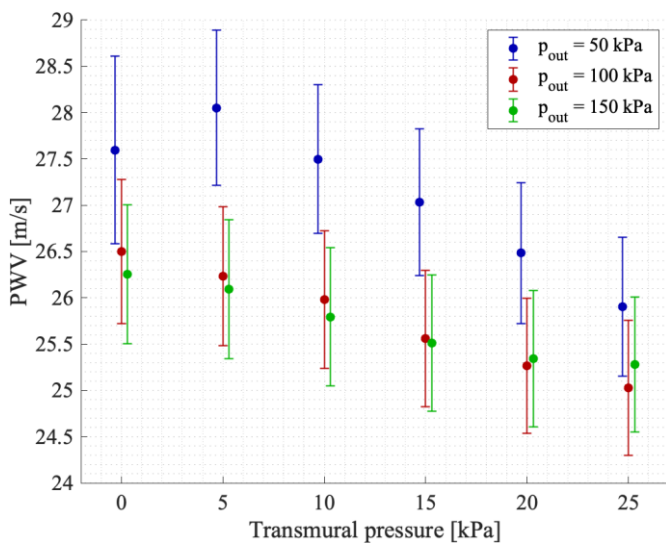


Figure 3. PWV values as a function of the transmural pressure.

REFERENCES

- [1] S. Laurent, P. Boutouyrie, R. Asmar, I. Gautier, B. Laloux, L. Guize, P. Ducimetiere, A. Benetos, Aortic stiffness is an independent predictor of all-cause and cardiovascular mortality in hypertensive patients, *Hypertension* 37 (2001) 5, pp. 1236-1241. DOI: [10.1161/01.hyp.37.5.1236](https://doi.org/10.1161/01.hyp.37.5.1236)
- [2] S. P. Glasser, D. K. Arnett, G. E. McVeigh, S. M. Finkelstein, A. J. Bank, D. J. Morgan, J. N. Cohn, Vascular compliance and cardiovascular disease: a risk factor or a marker?, *Am. J. Hypertens.* 10 (1997) 10, pp. 1175-1189. DOI: [10.1161/01.hyp.10.10.1175](https://doi.org/10.1161/01.hyp.10.10.1175)
- [3] H.-L. Kim, S.-H. Kim, Pulse wave velocity in atherosclerosis, *Front. Cardiovasc. Med.* 6 (2019) 41. DOI: [10.3389/fcvm.2019.00041](https://doi.org/10.3389/fcvm.2019.00041)
- [4] P. Boutouyrie, A. I. Tropeano, R. Asmar, I. Gautier, A. Benetos, P. Lacolley, S. Laurent, Aortic stiffness is an independent predictor of primary coronary events in hypertensive patients: a longitudinal study, *Hypertension* 39 (2002) 1, pp. 10-15. DOI: [10.1161/hy0102.099031](https://doi.org/10.1161/hy0102.099031)
- [5] G. E. McVeigh, C. W. Bratteli, D. J. Morgan, C. M. Alinder, S. P. Glasser, S. M. Finkelstein, J. N. Cohn, Age-related abnormalities in arterial compliance identified by pressure pulse contour analysis: aging and arterial compliance, *Hypertension* 33 (1999) 6, pp. 1392-1398. DOI: [10.1161/01.hyp.33.6.1392](https://doi.org/10.1161/01.hyp.33.6.1392)
- [6] P. K. Hamilton, C. J. Lockhart, C. E. Quinn, G. E. McVeigh, Arterial stiffness: clinical relevance, measurement and treatment, *Clin. Sci. (Lond.)* 113 (2007) 4, pp. 157-170. DOI: [10.1042/cs20070080](https://doi.org/10.1042/cs20070080)
- [7] World Health Organization, Cardiovascular diseases (CVDs). Online [Accessed 17 June 2024] <https://www.who.int/news-room/fact-sheets/detail/cardiovascular-diseases-cvds>
- [8] Y. C. Fung, *Biomechanics: Circulation*, New York, NY: Springer New York, 1997. DOI: [10.1007/978-1-4757-2696-1](https://doi.org/10.1007/978-1-4757-2696-1)
- [9] J. C. Bramwell, A. V. Hill, The velocity of pulse wave in man, *Proc. R. Soc. Lond. B.* 93 (1922) 652, pp. 298-306. DOI: [10.1098/rspb.1922.0022](https://doi.org/10.1098/rspb.1922.0022)
- [10] I. S. Mackenzie, I. B. Wilkinson, J. R. Cockcroft, Assessment of arterial stiffness in clinical practice, *QJM* 95 (2002) 2, pp.67-74. DOI: [10.1093/qjmed/95.2.67](https://doi.org/10.1093/qjmed/95.2.67)
- [11] S. Laurent, J. Cockcroft, L. Van Bortel, P. Boutouyrie, C. Giannattasio, D. Hayoz, B. Pannier, C. Vlachopoulos, I. Wilkinson, H. Struijker-Boudier, European Network for Non-invasive Investigation of Large Arteries, Expert consensus document on arterial stiffness: methodological issues and clinical applications, *Eur. Heart J.* 27 (2006) 21, pp. 2588-2605. DOI: [10.1093/eurheartj/ehl254](https://doi.org/10.1093/eurheartj/ehl254)
- [12] A. Milan, G. Zocaro, D. Leone, F. Tosello, I. Buraioli, D. Schiavone, F. Veglio, Current assessment of pulse wave velocity: comprehensive review of validation studies, *J. Hypertens.* 37 (2019) 8, pp.1547-1557. DOI: [10.1097/hjh.0000000000002081](https://doi.org/10.1097/hjh.0000000000002081)
- [13] G. Fiori, F. Fuiano, A. Scorza, S. Conforto, S. A. Sciuto, Non-invasive methods for PWV measurement in blood vessel stiffness assessment, *IEEE Rev. Biomed. Eng.* 15 (2022), pp.169-183. DOI: [10.1109/rbme.2021.3092208](https://doi.org/10.1109/rbme.2021.3092208)
- [14] S. G. Karr, Theoretical and experimental determination of arterial pulse propagation speed, Evanston, Ill., Northwestern University, 1982, PhD Thesis.
- [15] F. Filippi, G. Fiori, G. Bocchetta, S. A. Sciuto, A. Scorza, A preliminary comparison of three methods for the assessment of pulse wave transit time in an arterial simulator, *Proc. of the 26th IMEKO TC4 Symposium and 24th International Workshop on ADC and DAC Modelling and Testing (IWADC)*, Pordenone, Italy, 20 – 21 September 2023, pp. 186-189. DOI: [10.21014/tc4-2023.43](https://doi.org/10.21014/tc4-2023.43)
- [16] Y. C. Chiu, P. W. Arand, S. G. Shroff, T. Feldman, J. D. Carroll, Determination of pulse wave velocities with computerized algorithms, *Am. Heart J.* 121 (1991) 5, pp. 1460-1470. DOI: [10.1016/0002-8703\(91\)90153-9](https://doi.org/10.1016/0002-8703(91)90153-9)
- [17] S. C. Millasseau, A. D. Stewart, S. J. Patel, S. R. Redwood, P. J. Chowienzyk, Evaluation of carotid-femoral pulse wave velocity: Influence of timing algorithm and heart rate, *Hypertension* 45 (2005) 2, pp. 222-226. DOI: [10.1161/01.hyp.0000154229.97341.d2](https://doi.org/10.1161/01.hyp.0000154229.97341.d2)
- [18] M. Benthin, P. Dahl, R. Ruzicka, K. Lindström, Calculation of pulse-wave velocity using cross correlation—Effects of reflexes in the arterial tree, *Ultrasound Med. Biol.* 17 (1991) 5, pp. 461-469. DOI: [10.1016/0301-5629\(91\)90182-v](https://doi.org/10.1016/0301-5629(91)90182-v)
- [19] M. Dauzat, G. Deklunder, B. Adam, A. de Césaire, J. Ayoub, J. Massé-Biron, C. Préfaut, P. Péronneau, Pulse wave velocity measurement by cross-correlation of Doppler velocity signals. Application to elderly volunteers during training, *Int. J. Sports Med.* 17 (1996) 8, pp. 547-553. DOI: [10.1055/s-2007-972893](https://doi.org/10.1055/s-2007-972893)
- [20] S. W. Fielden, B. K. Fornwalt, M. Jerosch-Herold, R. L. Eisner, A. E. Stillman, J. N. Oshinski, A new method for the determination of aortic pulse wave velocity using cross-correlation on 2D PCMR velocity data, *J. Magn. Reson. Imaging* 27 (2008) 6, pp. 1382-1387. DOI: [10.1002/jmri.21387](https://doi.org/10.1002/jmri.21387)
- [21] Y. Wang, E. Estrada, N. Reichel, Detection of time delay using cross-correlation for aortic pulse wave velocity evaluation, *J. Cardiovasc. Magn. Reson.* 12 (2010) Suppl 1. DOI: [10.1186/1532-429X-12-S1-P144](https://doi.org/10.1186/1532-429X-12-S1-P144)
- [22] D. Bessems, C. G. Giannopapa, M. C. Rutten, F. N. van de Vosse, Experimental validation of a time-domain-based wave propagation model of blood flow in viscoelastic vessels, *J. Biomech.* 41 (2008) 2, pp. 284-291. DOI: [10.1016/j.jbiomech.2007.09.014](https://doi.org/10.1016/j.jbiomech.2007.09.014)
- [23] J. H. Olsen, A. H. Shapiro, Large-amplitude unsteady flow in liquid-filled elastic tubes, *J. Fluid Mech.* 29 (1967) 3, pp. 513-538. DOI: <https://doi.org/10.1017/S00222112067001004>
- [24] M. Gally, M. Güney, E. Rieutord, An investigation of pressure transients in viscoelastic pipes, *ASME J. Fluids Eng.* 101 (1979) 4, pp. 495-499. DOI: [10.1115/1.3449017](https://doi.org/10.1115/1.3449017)
- [25] L. Suo, E. B. Wylie, Complex wavespeed and hydraulic transients in viscoelastic pipes, *ASME J. Fluids Eng.* 112 (1990) 4, pp. 496-500. DOI: [10.1115/1.2909434](https://doi.org/10.1115/1.2909434)
- [26] M. Prek, Analysis of wave propagation in fluid-filled viscoelastic pipes, *MSSP* 21 (2007) 4, pp. 1907-1916. DOI: [10.1016/j.ymsp.2006.07.013](https://doi.org/10.1016/j.ymsp.2006.07.013)
- [27] F. Fuiano, A. Scorza, S. A. Sciuto, Functional and metrological issues in arterial simulators for biomedical testing applications: a review, *Metrology* 2 (2022) 3, pp. 360-386. DOI: [10.3390/metrology2030022](https://doi.org/10.3390/metrology2030022)
- [28] G. J. Langewouters, K. H. Wesseling, W. J. Goedhard, The static elastic properties of 45 human thoracic and 20 abdominal aortas in vitro and the parameters of a new model, *J. Biomech.* 17 (1984) 6, pp. 425-435. DOI: [10.1016/0021-9290\(84\)90034-4](https://doi.org/10.1016/0021-9290(84)90034-4)
- [29] G. J. Langewouters, K. H. Wesseling, W. J. Goedhard, The pressure dependent dynamic elasticity for 35 thoracic and 16 abdominal human aortas in vitro described by a five component model, *J. Biomech.* 18 (1985) 8, pp. 613-620. DOI: [10.1016/0021-9290\(85\)90015-6](https://doi.org/10.1016/0021-9290(85)90015-6)
- [30] G. J. Langewouters, A. Zwart, R. Busse, K. H. Wesseling, Pressure-diameter relationships of segments of human finger arteries, *Clin. Phys. Physiol. Meas.* 7 (1986) 1, pp. 43-56. DOI: [10.1088/0143-0815/7/1/003](https://doi.org/10.1088/0143-0815/7/1/003)
- [31] G. Fiori, F. Fuiano, S. Conforto, S. A. Sciuto, A. Scorza, A novel equivalent time sampling-based method for pulse transit time estimation with applications into the cardiovascular disease diagnosis, *Sensors* 23 (2023). DOI: [10.3390/s23115005](https://doi.org/10.3390/s23115005)

- [32] F. Fuiano, G. Fiori, A. Scorza, S. A. Sciuto, A novel experimental set-up for Young modulus assessment through transit time measurements in biomedical applications, Proc. of the 2021 IEEE Int. Workshop on Metrology for Industry 4.0 & IoT (MetroInd4.0&IoT), Rome, Italy, 7 – 9 June 2021. DOI: [10.1109/MetroInd4.0IoT51437.2021.9488460](https://doi.org/10.1109/MetroInd4.0IoT51437.2021.9488460)
- [33] F. Fuiano, G. Fiori, F. Vurchio, A. Scorza, S. A. Sciuto, Transit time measurement of a pressure wave through an elastic tube based on LVDT sensors, Proc. of the 24th IMEKO TC4 Int. Symp. & 22nd Int. Workshop on ADC and DAC Modelling and Testing, IMEKO TC4 2020, Palermo, Italy, 14 – 16 September 2020. Online [Accessed 17 June 2024] <https://www.imeko.org/publications/tc4-2020/IMEKO-TC4-2020-60.pdf>
- [34] F. Filippi, G. Fiori, G. Bocchetta, S. A. Sciuto, A. Scorza, First experimental results of a novel arterial simulator with PWV adjustment, Proc. of the 26th IMEKO TC4 Symp. and 24th Int. Workshop on ADC and DAC Modelling and Testing (IWADC), Pordenone, Italy, 20 – 21 September 2023, pp. 170-173. DOI: [10.21014/tc4-2023.39](https://doi.org/10.21014/tc4-2023.39)
- [35] F. Gustafsson, Determining the initial states in forward-backward filtering, IEEE Trans. Signal Process. 44 (1996) 4, pp. 988-992. DOI: [10.1109/78.492552](https://doi.org/10.1109/78.492552)
- [36] G. Fiori, G. Bocchetta, S. Conforto, S. A. Sciuto, A. Scorza, Sample volume length and registration accuracy assessment in quality controls of PW Doppler diagnostic systems: a comparative study, Acta IMEKO 12 (2023) 2, pp. 1-7. DOI: [10.21014/actaimeko.v12i2.1425](https://doi.org/10.21014/actaimeko.v12i2.1425)
- [37] G. Fiori, G. Bocchetta, M. Schmid, S. Conforto, S. A. Sciuto, A. Scorza, Novel quality assessment protocol based on Kiviat diagram for pulsed wave Doppler diagnostic systems: first results, Proc. of the 26th IMEKO TC4 Int. Symp. & 24th Int. Workshop on ADC and DAC Modelling and Testing (IWADC), Pordenone, Italy, 20 – 21 September 2023, pp. 165-169. DOI: [10.21014/tc4-2023.38](https://doi.org/10.21014/tc4-2023.38)
- [38] M. De Cecco, A. Luchetti, M. Tavernini, Monte Carlo human identification refinement using joints uncertainty, Acta IMEKO 12 (2023) 2, pp. 1-11. DOI: [10.21014/actaimeko.v12i2.1423](https://doi.org/10.21014/actaimeko.v12i2.1423)
- [39] N. Covre, A. Luchetti, M. Lancini, S. Pasinetti, E. Bertolazzi, M. De Cecco, Monte Carlo-based 3D surface point cloud volume estimation by exploding local cubes faces, Acta IMEKO 11 (2022) 2, pp. 1-9. DOI: [10.21014/actaimeko.v11i2.1206](https://doi.org/10.21014/actaimeko.v11i2.1206)
- [40] P. C. Chang, A. Lin, G. A. Secor, K. S. Su, Determination of the pulse wave velocity by a filtered cross-correlation technique, J. Biomech. 4 (1971) 6, pp. 579-587. DOI: [10.1016/0021-9290\(71\)90047-9](https://doi.org/10.1016/0021-9290(71)90047-9)
- [41] N. R. Gaddum, J. Alastruey, P. Beerbaum, P. Chowienzyk, T. Schaeffter, A technical assessment of pulse wave velocity algorithms applied to non-invasive arterial waveforms, Ann. Biomed. Eng. 41 (2013) 12, pp. 2617-2629. DOI: [10.1007/s10439-013-0854-y](https://doi.org/10.1007/s10439-013-0854-y)
- [42] J. R. Taylor, An introduction to error analysis: the study of uncertainties in physical measurements, 2. ed. Sausalito, Calif: University Science Books, 1997.
- [43] P. Nauleau, I. Apostolakis, M. McGarry, E. Konofagou, Cross-correlation analysis of pulse wave propagation in arteries: in vitro validation and in vivo feasibility, Phys. Med. Biol. 63 (2018) 11. DOI: [10.1088/1361-6560/aabe57](https://doi.org/10.1088/1361-6560/aabe57)
- [44] A. Spagnoli, M. Terzano, R. Brighenti, F. Artoni, A. Carpinteri, How soft polymers cope with cracks and notches, Applied Sciences 9 (2019) 6. DOI: [10.3390/app9061086](https://doi.org/10.3390/app9061086)